Electronic Supplementary Material (ESI) for Analytical Methods.
This journal is © The Royal Society of Chemistry 2019

Supporting Information

Disposable electrochemical biosensor based on surface-modified screen-printed electrodes for organophosphorus pesticide analysis

Quoc Trung Hua[a], Nipapan Ruecha[b], Yuki Hiruta, Daniel Citterio[a]*

[a] *Department of Applied Chemistry, Faculty of Science and Technology, Keio University, 3-14-1, Hiyoshi, Kohoku-ku, Yokohama 223-8522, Japan*

[b] *Metallurgy and Materials Science Research Institute, Chulalongkorn University, Soi Chula 12, Phyathai Road, Patumwan, Bangkok 10330, Thailand*

[†]*To whom correspondence should be addressed.
E-mail: citterio@applc.keio.ac.jp; Phone: +81 45 566 1568; Fax: +81 45 566 1568

Table of contents

Supplementary figures:

Fig. S1: Photograph of an as received screen-printed electrode 3
Fig. S2: Preparation of spinach samples 4
Fig. S3: Reaction mechanism based on AChE-catalyzed hydrolysis of ATCh 5
Fig. S4: MWCNTs-COOH dispersed in chitosan solution 6
Fig. S5: Optimization of electrochemical AuNPs deposition time 7
Fig. S6: Optimization of amount of MWCNTs-CS 8
Fig. S7: Optimization of ATCh and $K_3[Fe(CN)_6]$ concentrations 9
Fig. S8: Optimization of incubation time for the enzymatic reaction 10
Fig. S9: Optimization of the sensor operating potential 11
Fig. S10: Optimization of pH values for the enzymatic reaction 12
Fig. S11: Optimization of inhibition time 13

Fig. S12: Evaluation of the device-to-device reproducibility of the developed biosensors 14
Fig. S13: Chromatogram and calibration curve obtained by UV-HPLC analysis 15
Fig. S14: Paraoxon-ethyl response curves recorded in spinach matrix……16

Fig. S1: Photograph of an as received screen-printed electrode sensor with the three electrode configuration (counter electrode, working electrode, and reference electrode).

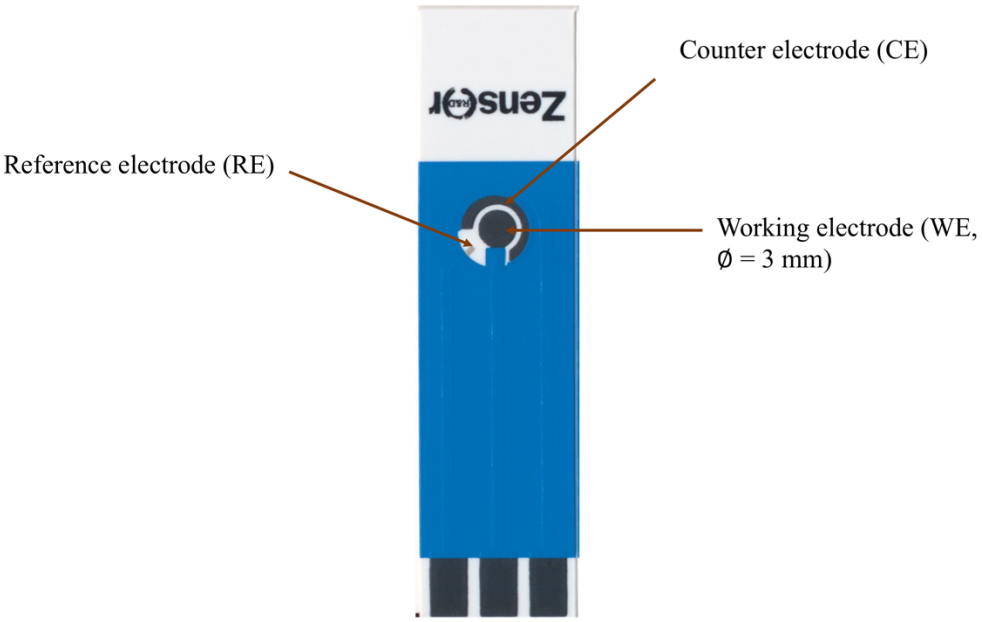

Fig. S2: Preparation of spinach samples: (a) image of cut spinach leaves and (b) obtained supernatant used for paraoxon-ethyl spiking.

Fig. S3: Reaction mechanism based on AChE-catalyzed hydrolysis of ATCh using ferricyanide as a redox mediator.

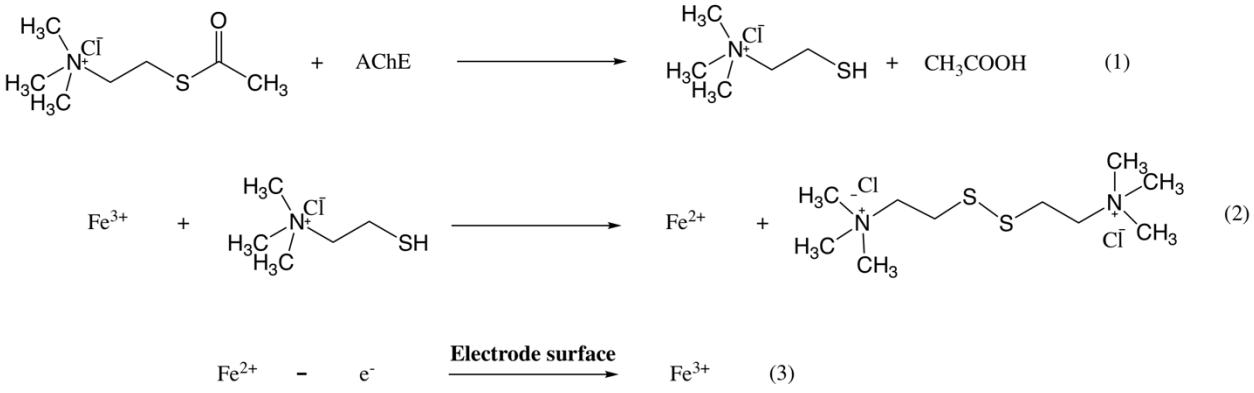

Fig. S4: Homogeneous dispersion of MWCNTs-COOH in 0.4% (v/v) chitosan obtained by sonication at 55°C for 6 hours.

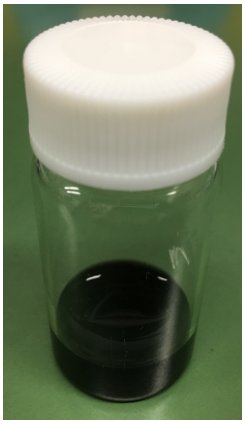

Fig. S5: Optimization of electrochemical AuNPs deposition time (0; 60; 120; 180 s) at a potential of - 0.4 V; 6 µL of 10 U/mL AChE pre-dried on the electrodes after AuNP deposition; current measurement at 0.4 V after application of 40 µL of 8 mM ATCh and 3 mM $K_3[Fe(CN)_6]$ solution in 50 mM phosphate buffer (pH 7.0) containing 0.1 M KCl after 35 min incubation; error bars represent standard deviations for measurements with 3 individual single-use biosensors.

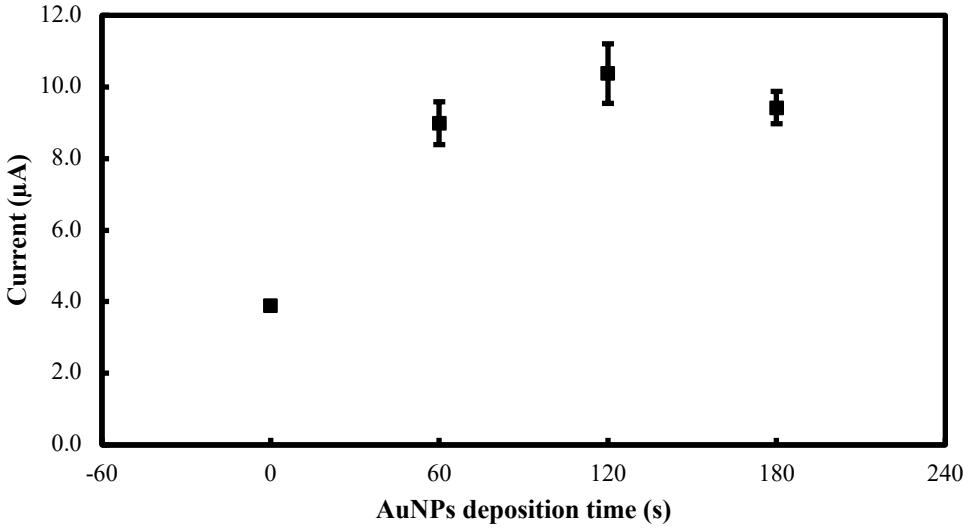

Fig. S6: Optimization of MWCNTs-CS (1 mg/mL) dispersion volume (2; 4; 6; 8; 10 μL) used for drop-casting onto AuNPs/SPCE; current measurement at 0.4 V with AChE/MWCNTs-CS/AuNPs/SPCEs (6 μL of 10 U/mL AChE pre-dried on the electrodes) after application of 40 μL of 8 mM ATCh and 3 mM $K_3[Fe(CN)_6]$ solution in 50 mM phosphate buffer (pH 7.0) containing 0.1 M KCl after 35 min incubation; error bars represent standard deviations for measurements with 3 individual single-use biosensors.

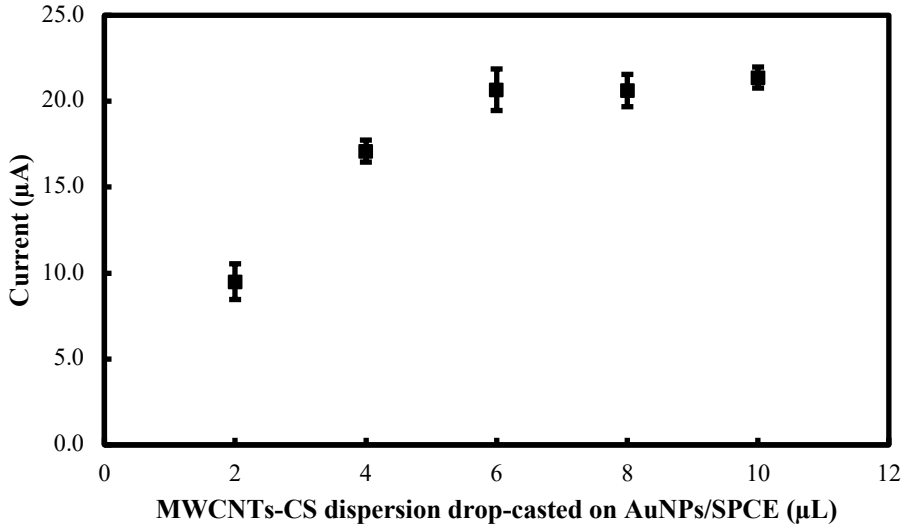

Fig. S7: a) Optimization of ATCh concentrations (6, 7, 8, 9 mM) and $K_3[Fe(CN)_6]$ concentrations (2, 3, 4 mM); current measurement at 0.4 V with AChE/MWCNTs-CS/AuNPs/SPCEs (6 µL of 10 U/mL AChE pre-dried on the electrodes) after application of 40 µL solutions of ATCh and $K_3[Fe(CN)_6]$ in 50 mM phosphate buffer (pH 7.0) containing 0.1 M KCl after 35 min incubation; error bars represent standard deviations for measurements with 3 individual single-use biosensors. b) Comparison in amperometric response of AChE/MWCNTs-CS/AuNPs/SPCEs in the presence or absence of 3 mM $K_3[Fe(CN)_6]$; other experimental conditions as mentioned for a).

A

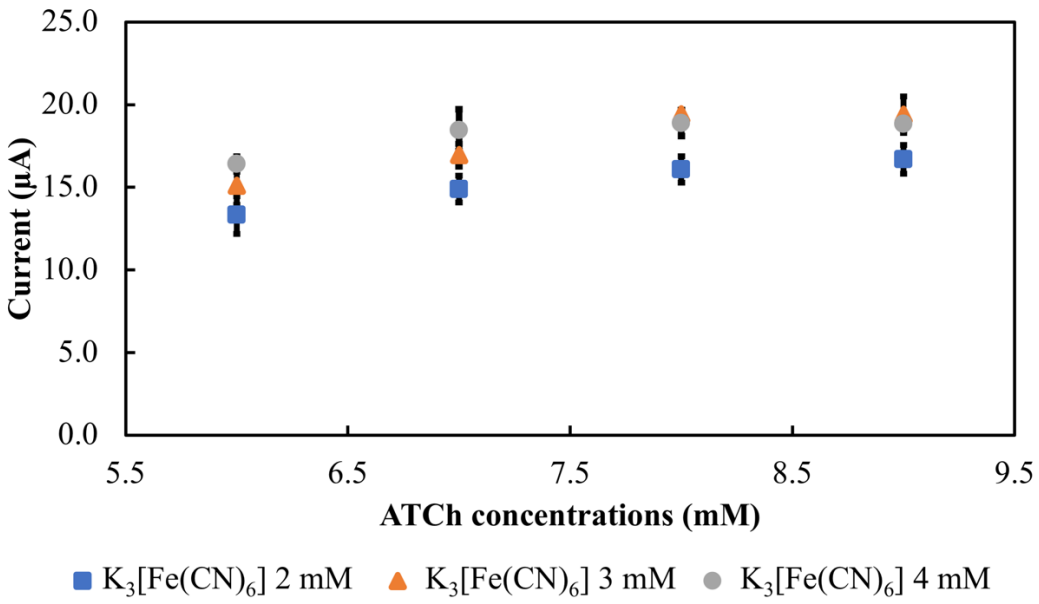

B

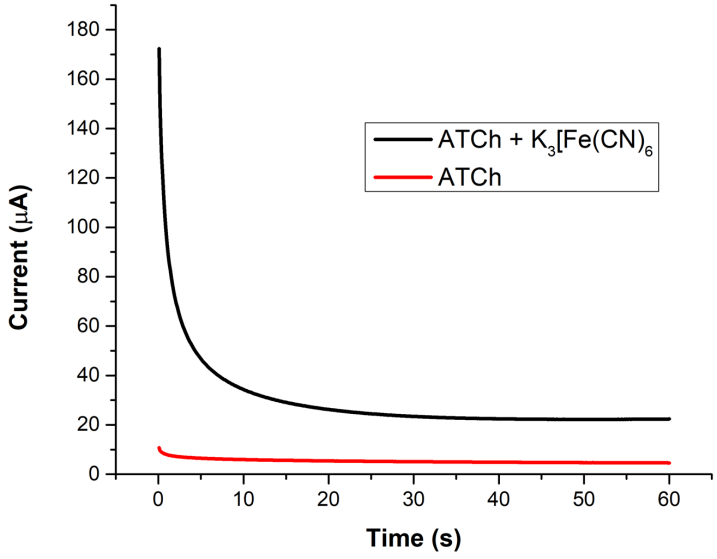

Fig. S8: Optimization of incubation time (5; 10; 15; 20; 25; 30; 35; 40; 45 min) for the enzymatic conversion of ATCh to electrochemically active thiocholine; current measurement at 0.4 V with AChE/MWCNTs-CS/AuNPs/SPCEs (6 µL of 10 U/mL AChE pre-dried on the electrodes) after application of 40 µL solutions of 8 mM ATCh and 3 mM $K_3[Fe(CN)_6]$ in 50 mM phosphate buffer (pH 7.0) containing 0.1 M KCl; error bars represent standard deviations for measurements with 3 individual single-use biosensors.

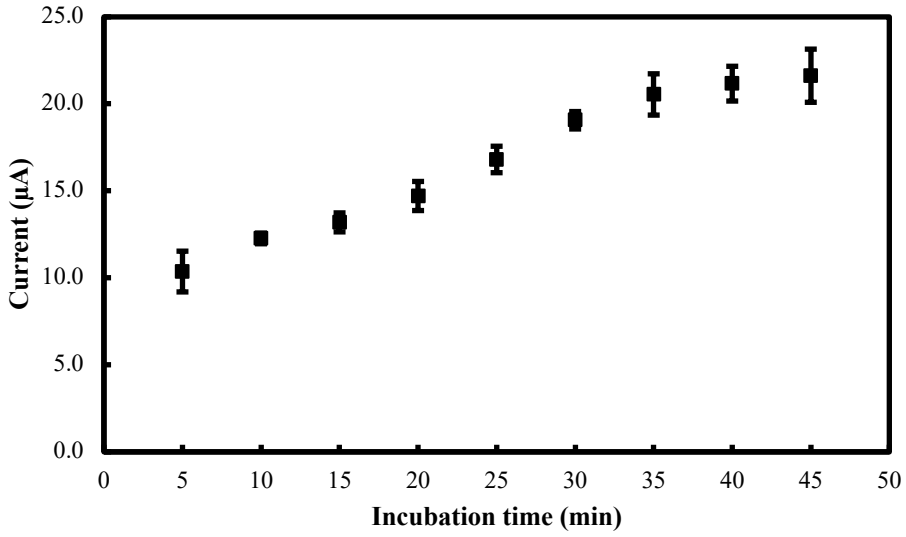

Fig. S9: Optimization of the applied potential for the oxidation of ferrocyanide to ferricyanide (0.1; 0.2; 0.3; 0.4; 0.5; 0.6 V); current measurement with AChE/MWCNTs-CS/AuNPs/SPCEs (6 µL of 10 U/mL AChE pre-dried on the electrodes) after application of 40 µL solutions of 8 mM ATCh and 3 mM $K_3[Fe(CN)_6]$ in 50 mM phosphate buffer (pH 7.0) containing 0.1 M KCl after 35 min incubation; error bars represent standard deviations for measurements with 3 individual single-use biosensors.

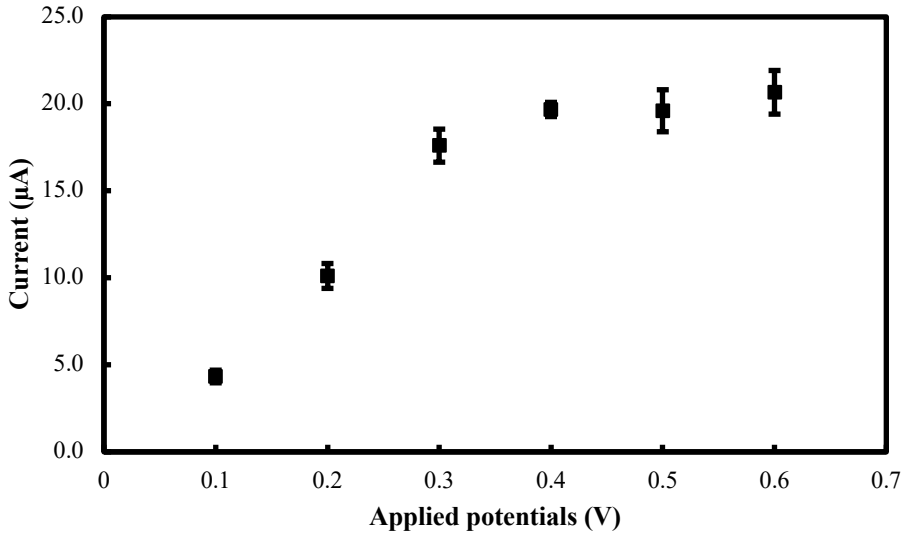

Fig. S10: Optimization of pH values (4; 5; 6; 7; 8; 9; 10) for the enzymatic reaction; current measurement at 0.4 V with AChE/MWCNTs-CS/AuNPs/SPCEs (6 μL of 10 U/mL AChE pre-dried on the electrodes) after application of 40 μL solutions of 8 mM ATCh and 3 mM $K_3[Fe(CN)_6]$ in 50 mM phosphate buffer of varying pH containing 0.1 M KCl after 35 min incubation; error bars represent standard deviations for measurements with 3 individual single-use biosensors.

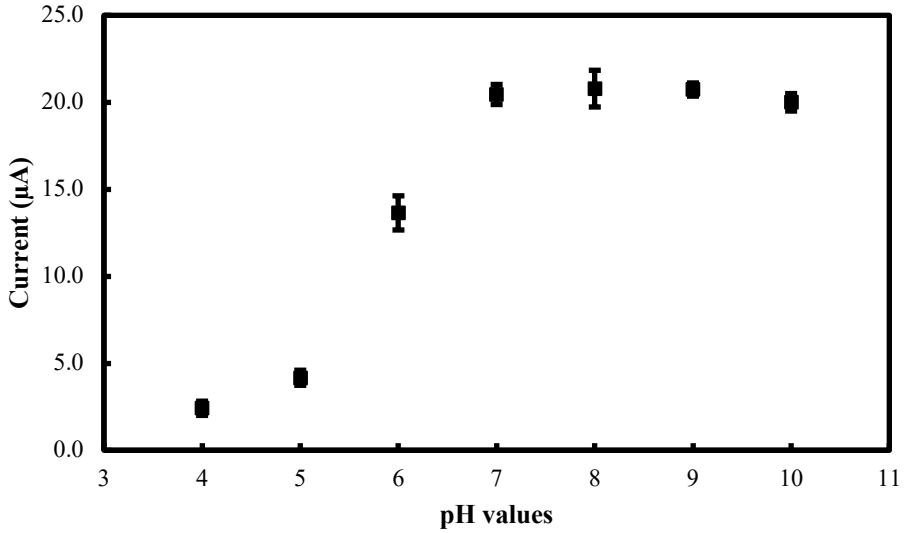

Fig. S11: Optimization of inhibition time (5; 10; 15; 20; 30; 40 min) for the inhibition of AChE by paraoxon-ethyl pesticide (40 μg/L); current measurements at 0.4 V with AChE/MWCNTs-CS/AuNPs/SPCEs (6 μL of 10 U/mL AChE pre-dried on the electrodes) after application of 40 μL solutions of 8 mM ATCh and 3 mM $K_3[Fe(CN)_6]$ in 50 mM phosphate buffer (pH 7.0) containing 0.1 M KCl after 35 min incubation; error bars represent standard deviations for measurements with 3 individual single-use biosensors.

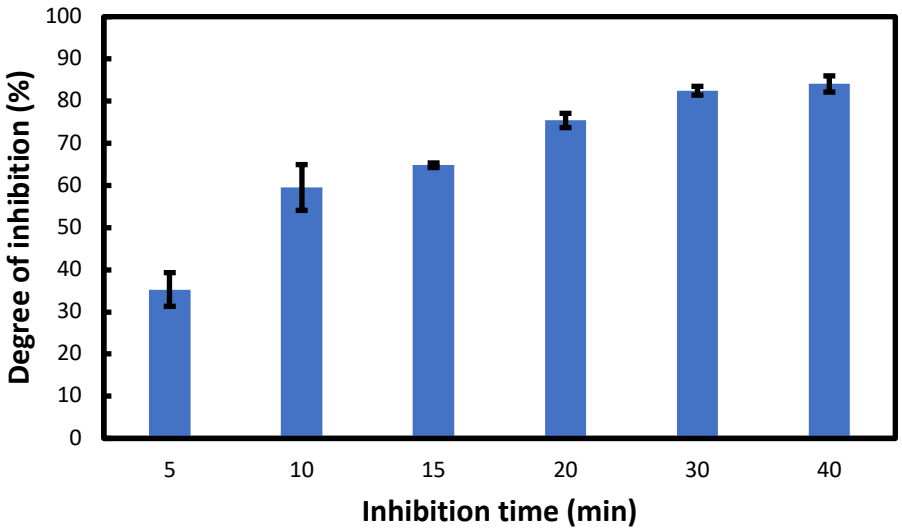

Fig. S12: Device-to-device fabrication reproducibility evaluation of the developed biosensors by current measurements after exposure to 20 μL of 10 μg/L paraoxon-ethyl; current measurement at 0.4 V with AChE/MWCNTs-CS/AuNPs/SPCEs (6 μL of 10 U/mL AChE pre-dried on the electrodes) after application of 40 μL solutions of 8 mM ATCh and 3 mM $K_3[Fe(CN)_6]$ in 50 mM phosphate buffer (pH 7.0) containing 0.1 M KCl after 35 min incubation.

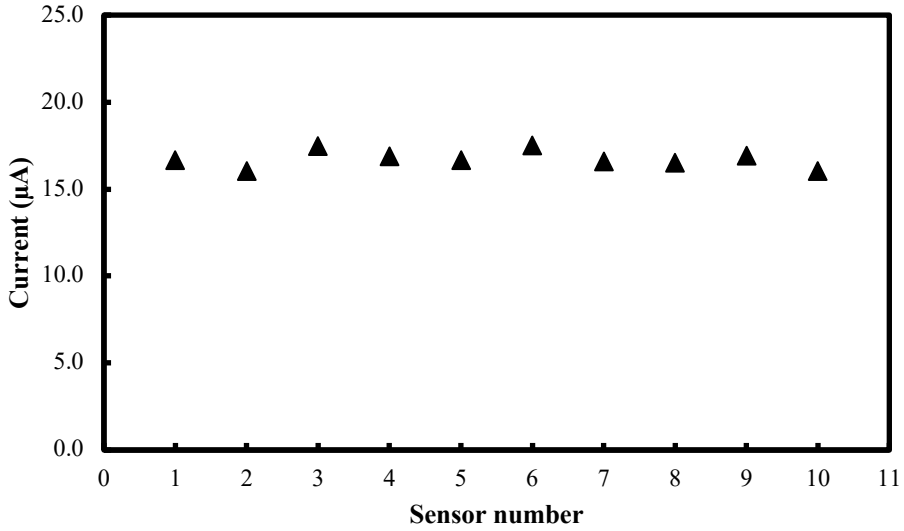

Fig. S13: Chromatograms (a) and calibration curve for paraoxon-ethyl (b) obtained by UV-HPLC analysis on a Prominence-i LC-2030C (Shimadzu, Kyoto, Japan) equipped with a COSMOSIL 3 C_{18}-MS-II Packed Column (ID = 2.0 mm, column length = 50 mm, NACALAI TESQUE, INC., Kyoto, Japan) with signal detection at 275 nm wavelength using 50% (v/v) aqueous methanol as a mobile phase.

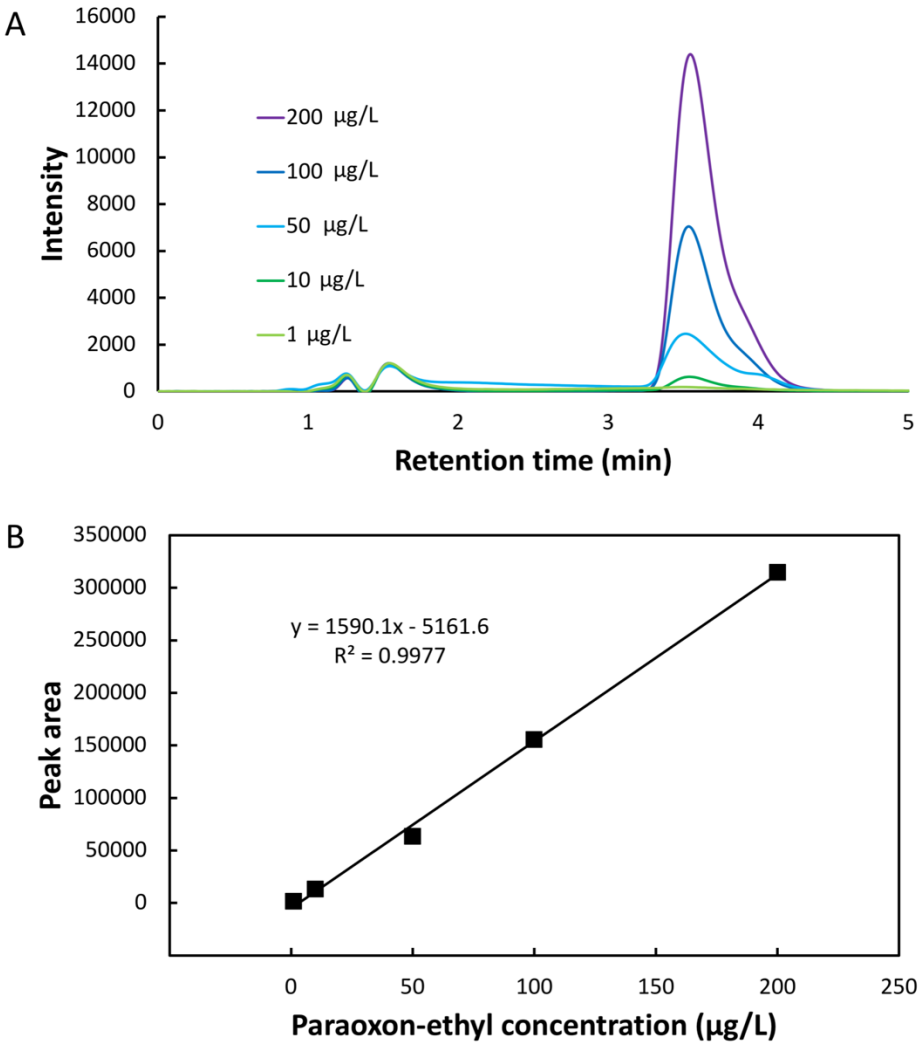
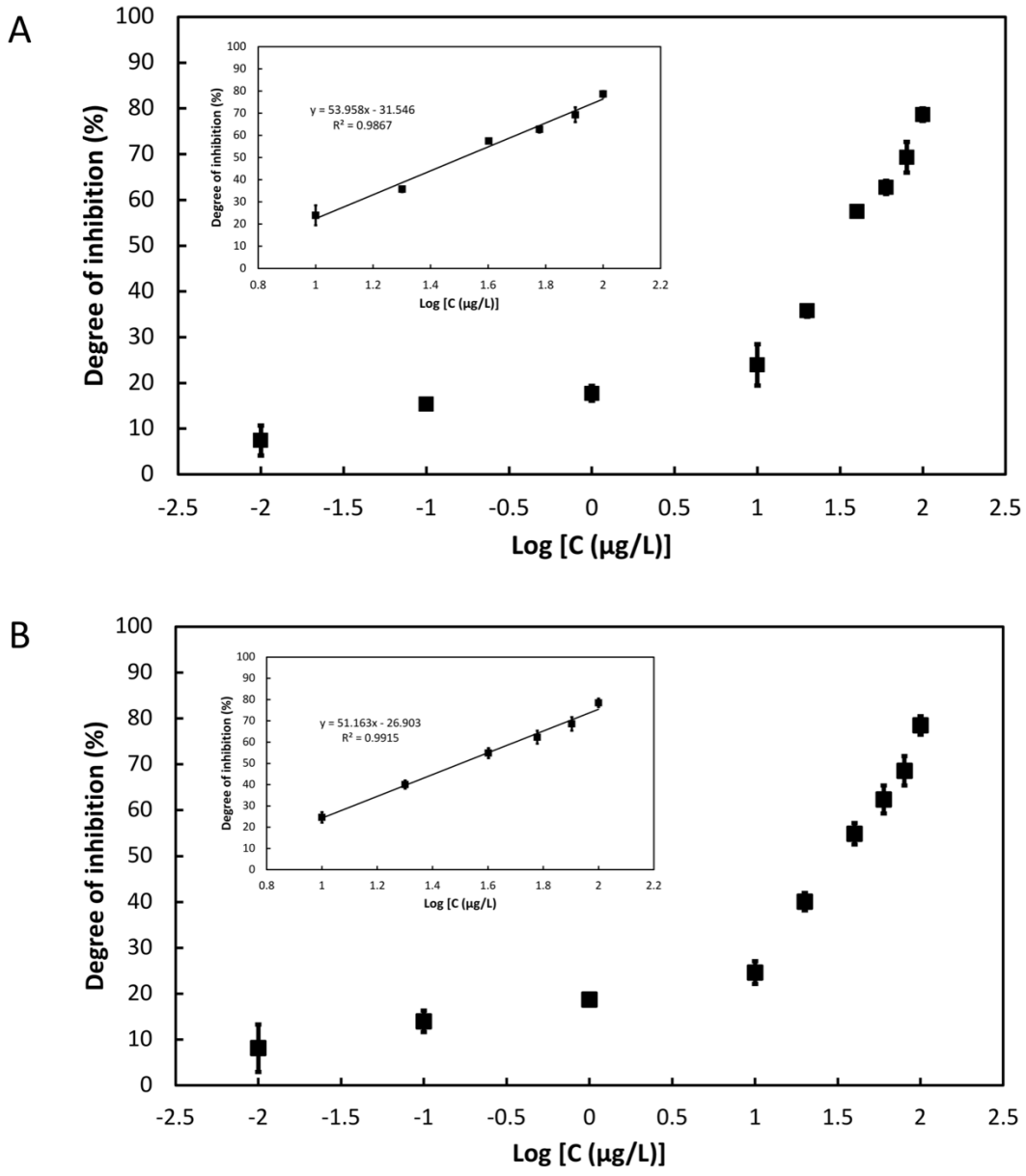
Fig. S14: Response curve obtained in the paraoxon-ethyl concentration range from 0 to 100 µg/L prepared in (a) 6% (v/v) aqueous ethanol and in (b) spinach sample matrix (see Fig. S2) containing 6% (v/v) aqueous ethanol; 10 min inhibition time; AChE (6 µL, 10 U/mL) pre-dried on the electrodes; added volume: 40 µL of 8 mM ATCh and 3 mM $K_3[Fe(CN)_6]$ solution in 50 mM phosphate buffer (pH 7.0), KCl 0.1 M; MWCNTs-CS (1 mg/mL) volume: 6 µL; AuNPs deposition time: 120 s; incubation time: 35 min; applied voltage: 0.4 V; error bars represent standard deviations for measurements with 3 individual single-use biosensors.